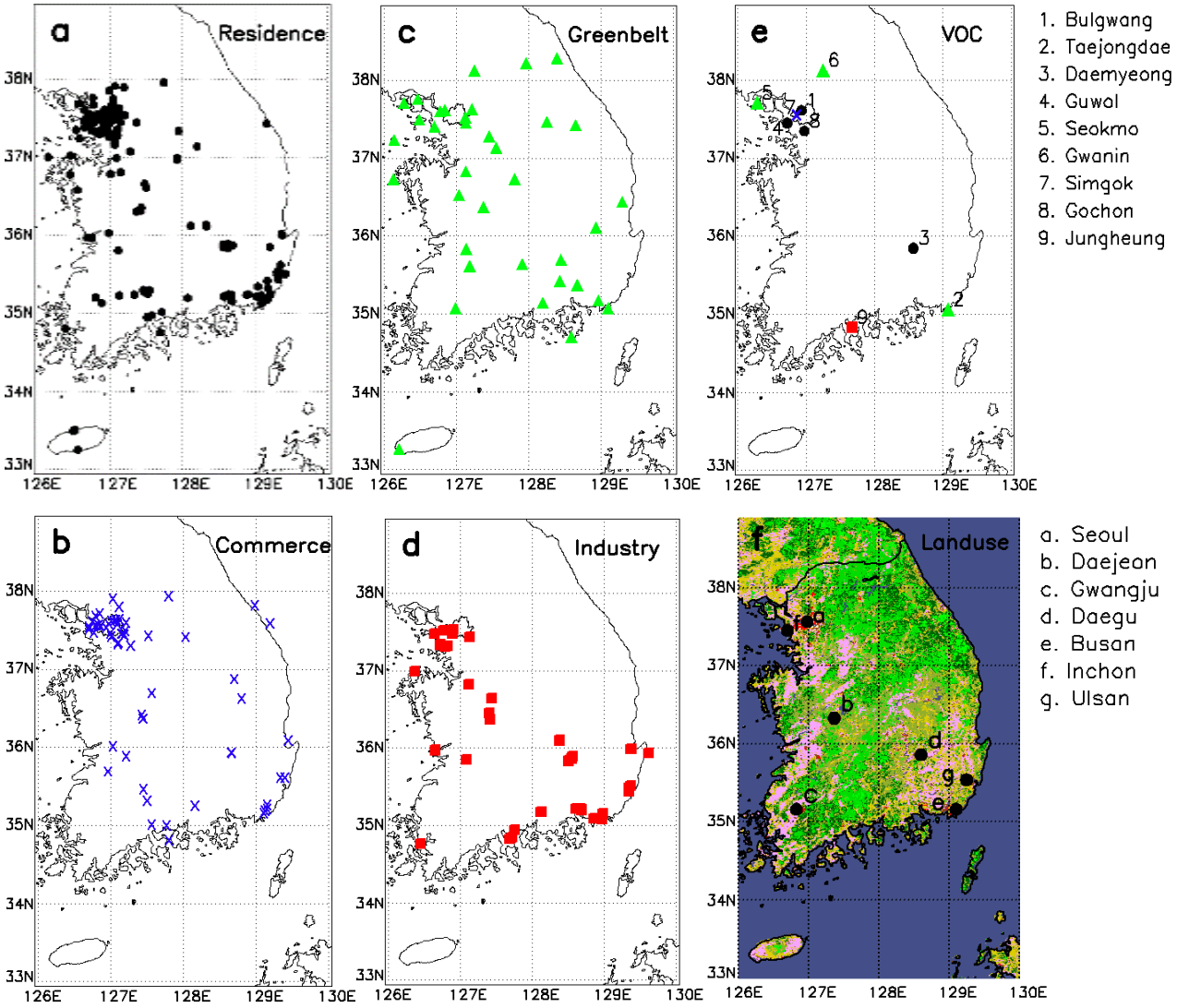

Fig. 1. Locations of surface air pollution (O_3, CO, NO_2, SO_2, and PM_{10}) monitoring stations in South Korea during 2002-2013 under the MEK four land-use types of a) residence (black circle), b) commerce (blue cross), c) greenbelt (green triangle) and d) industry (red square). e) Locations of the VOC monitoring stations, used in this study, under the four land-use types. f) Locations of seven major cities in South Korea with the satellite drived AVHRR land-cover types . The VOCs and the five kinds of air pollutants were simultaneously measured at the nine stations in Fig. 1e. Please see Table 1 for the observational periods of VOCs.

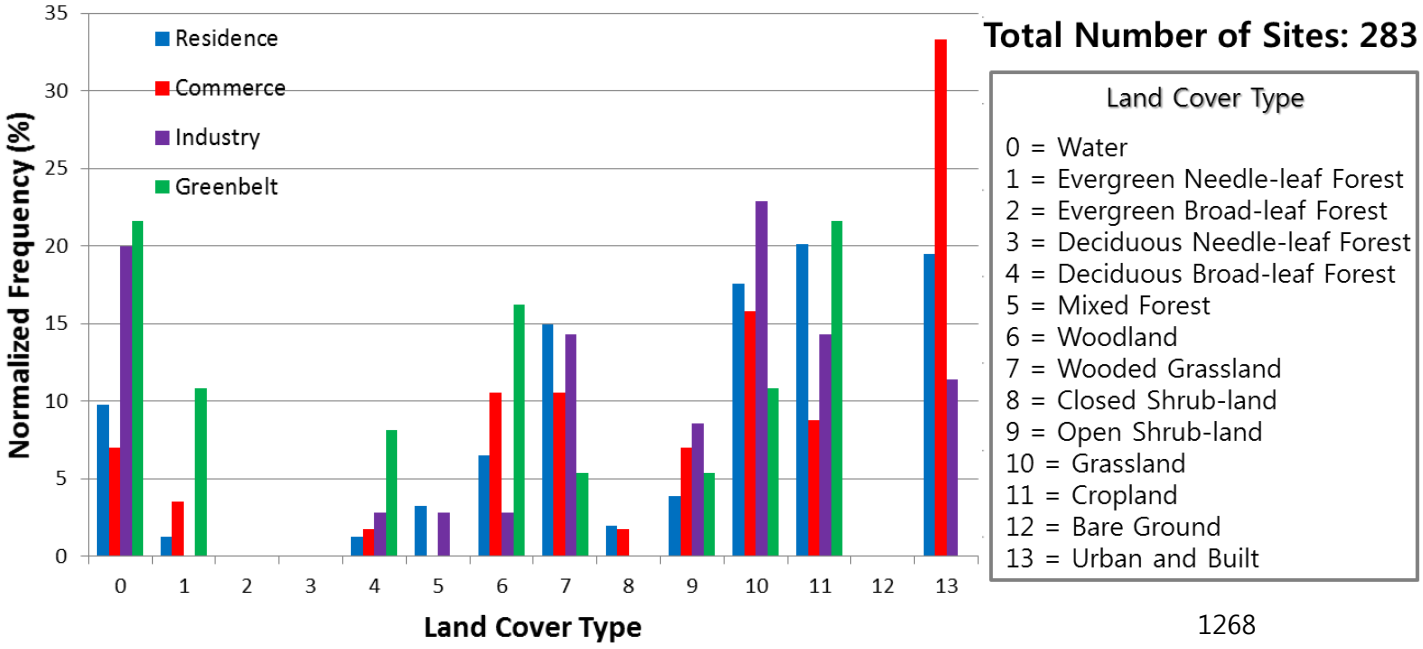

Fig. 2. Satellite-derived AVHRR land-cover types with respect to the MEK four land-use types (residence, commerce, industry and greenbelt) of 283 air pollution monitoring stations of the MEK in South Korea. The 13 AVHRR types were given at a 1km x 1km pixel resolution (e.g., De Fries et al., 1998; Hansen et al., 2000).

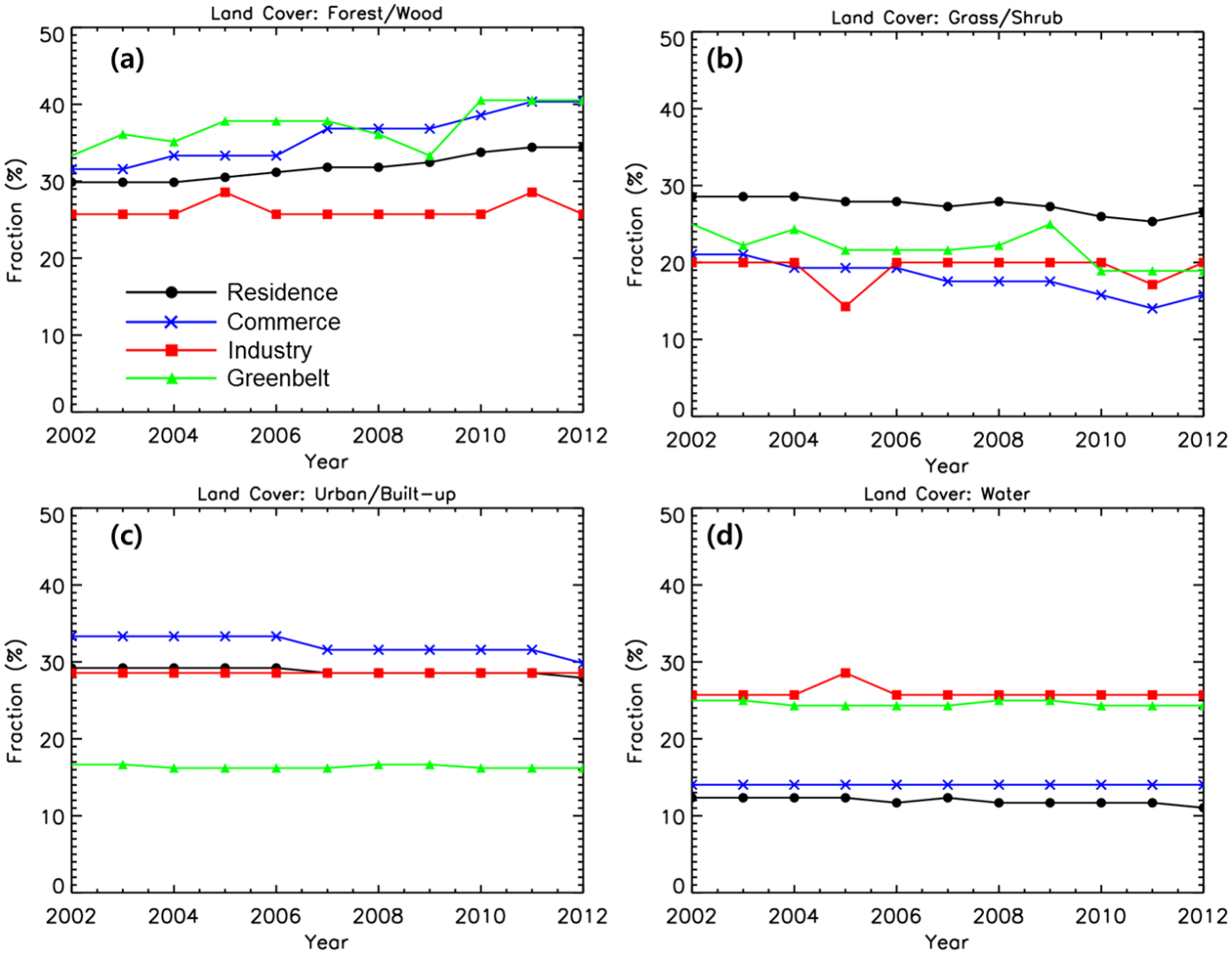

Fig. 3. Interannual variations of the satellite-derived MODIS land-cover types (%) versus the MEK four land-use types (residence, commerce, industry and greenbelt) of the 283 air pollution monitoring stations in South Korea during 2002-2012. In this study, for ease of comparison, the MODIS original types were regrouped into the following four covers; forest/wood, green/shrub, urban/built-up and water.

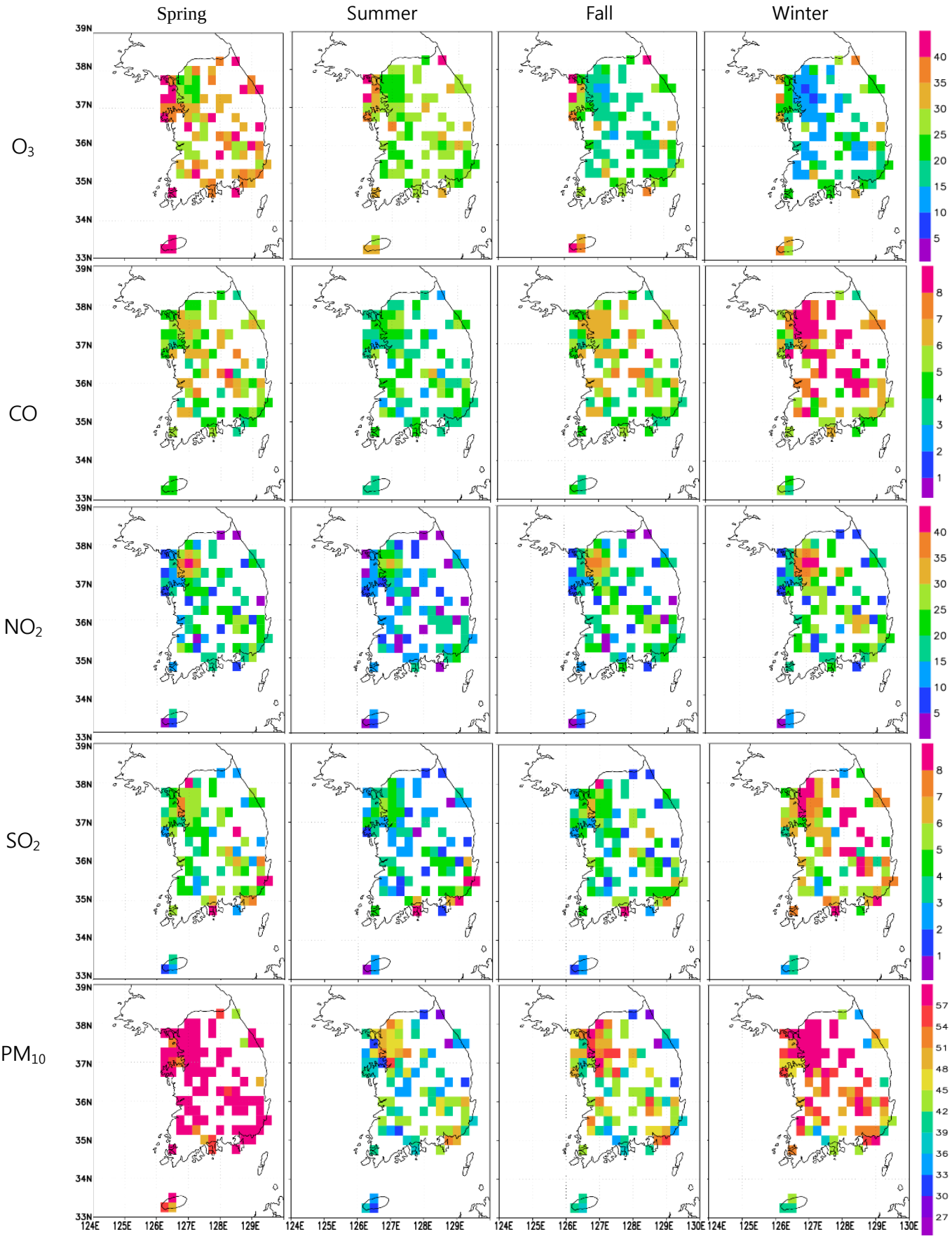

Fig. 4. Climatological seasonal averages of O_3 (ppb), CO (0.1 ppm), SO_2 (ppb), NO_2 (ppb), and PM_{10} ($\mu g m^{-3}$) in a 0.25° x 0.25°grid over South Korea during 2002-2013.

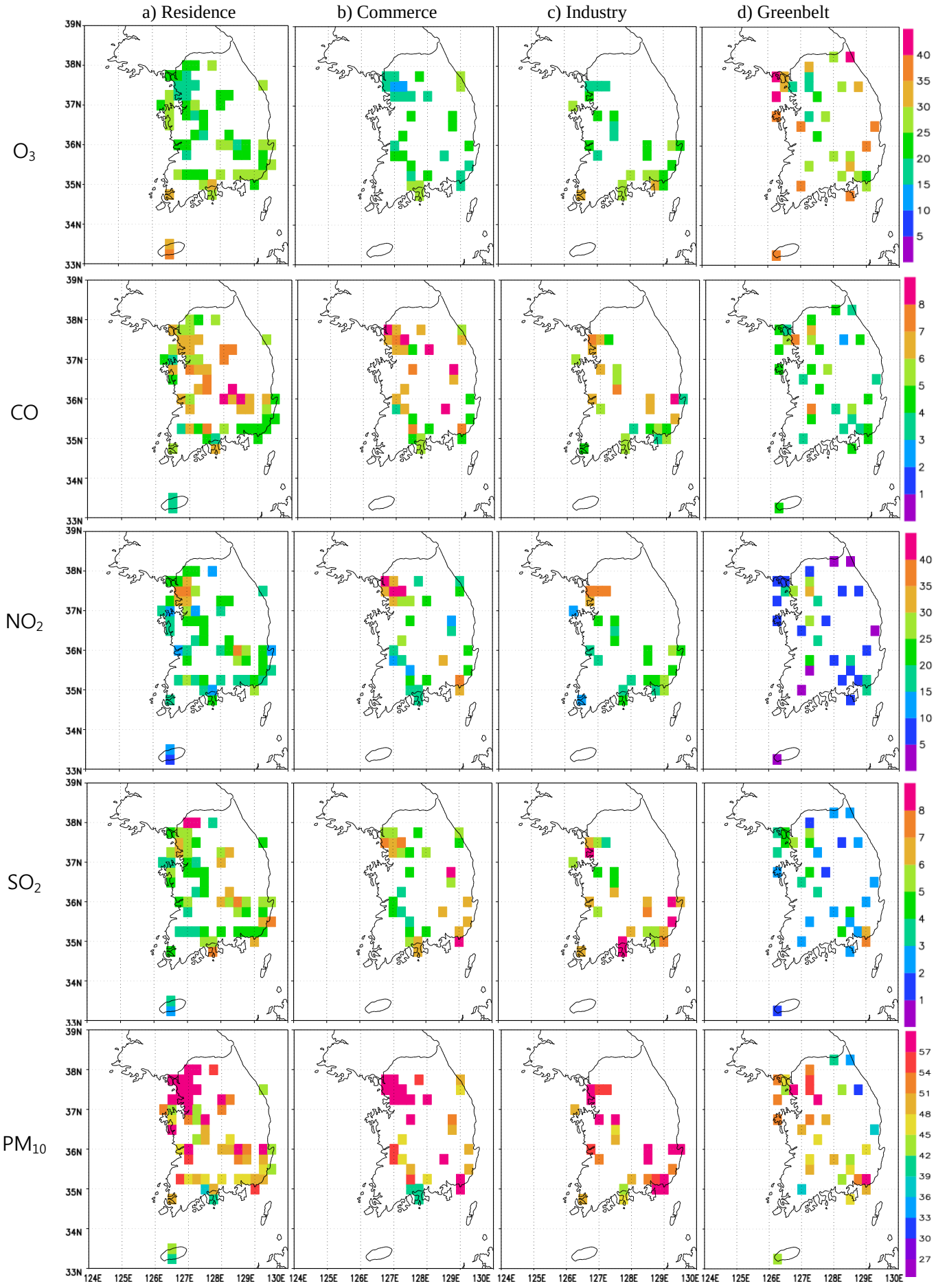

Fig. 5. Climatological annual averages in a 0.25°×0.25° grid over South Korea during 2002-2013 of the surface air pollutant observations of O_3 (ppb), CO (0.1ppm), NO_2 (ppb), SO_2 (ppb), and PM_{10}($\mu g\ m^{-3}$) under the MEK four land-use types of a) residence, b) commerce, c) industry, and d) greenbelt.

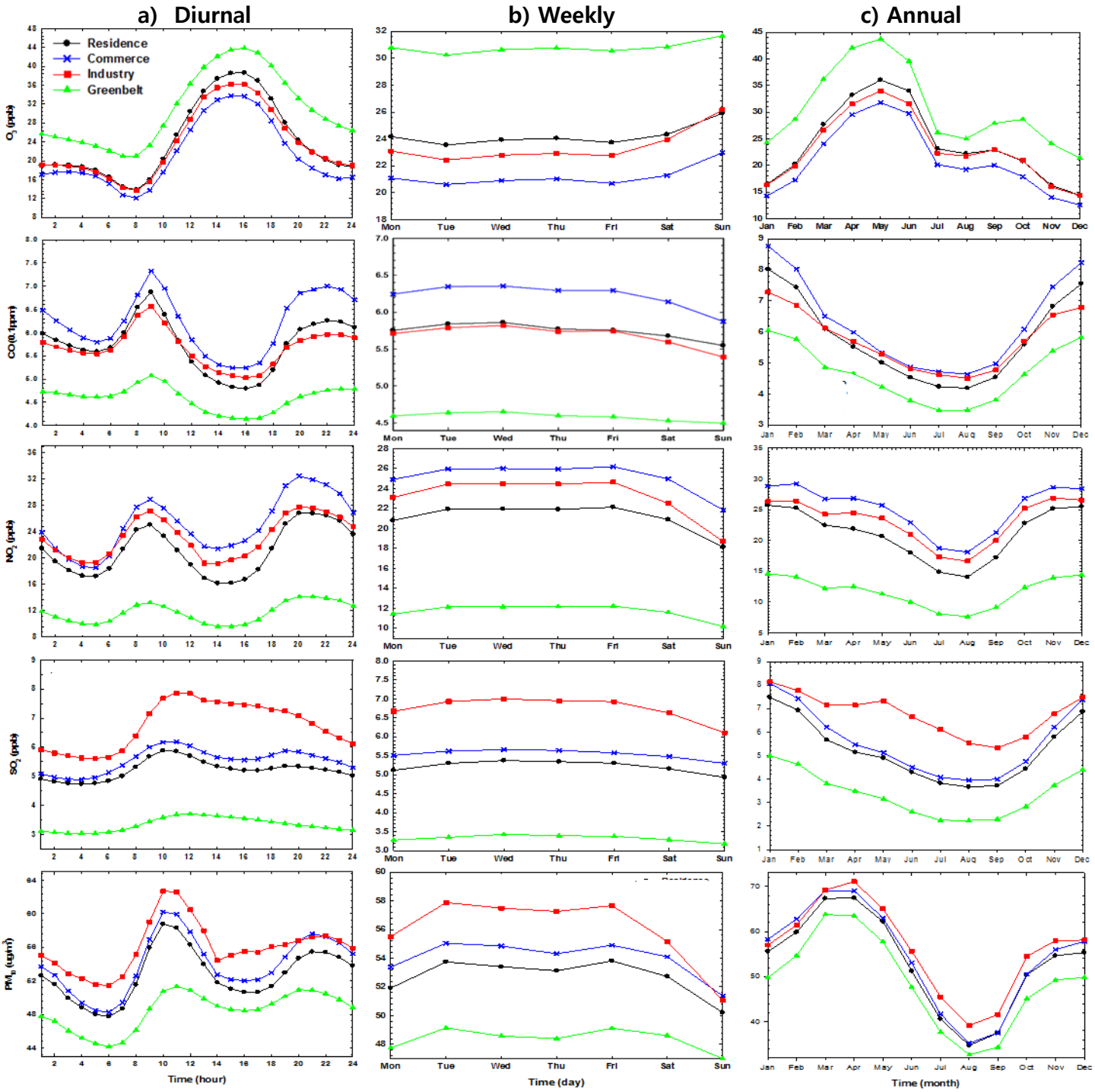

Fig. 6. The (a) diurnal, (b) weekly, and (c) annual variations in a 0.25°×0.25° grid of the O_3 (ppb), CO (0.1ppm), NO (ppb), SO_2, (ppb) and PM_{10} ($\mu g\ m^{-3}$) observations over South Korea during 2002-2013 under the MEK four land-use types as follows: residence (black circle), commerce (blue cross), industry (red square) and greenbelt (green triangle).

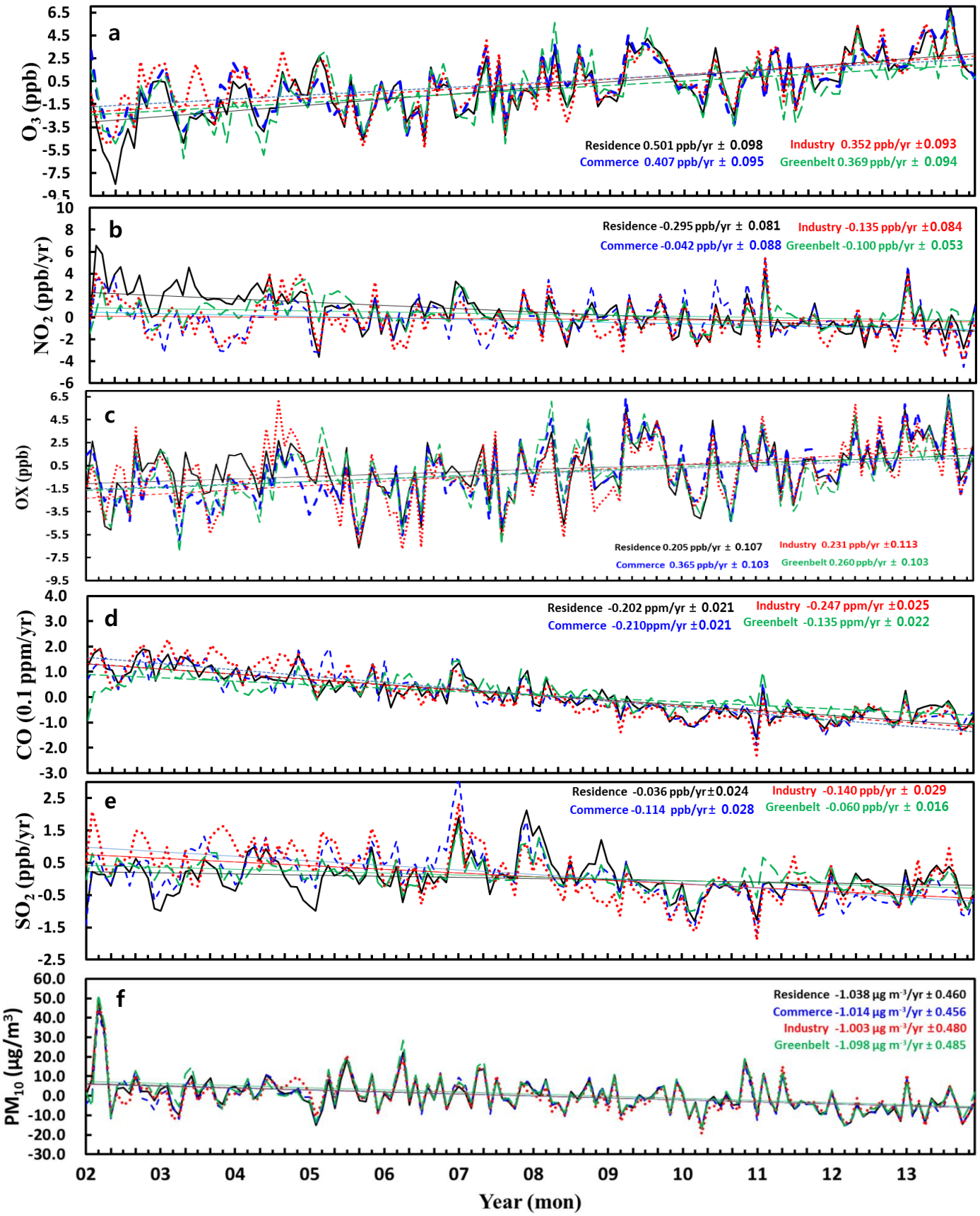

Fig. 7. Time series of the monthly surface air pollutant anomalies in a 0.25°×0.25° grid of the (a) O_3 (ppb), (b) NO_2 (ppb) (c) OX (ppb), (d) CO (0.1ppm), (e) SO_2 (ppb), and (f) PM_{10} (μgm^{-3}) observations over South Korea during the period from January 2002 to December 2013 under the following MEK land-use types; residence (black solid), commerce (blue dashed), industry (red dotted) and greenbelt (green dashed). The ± trend values define the 95% confidence intervals

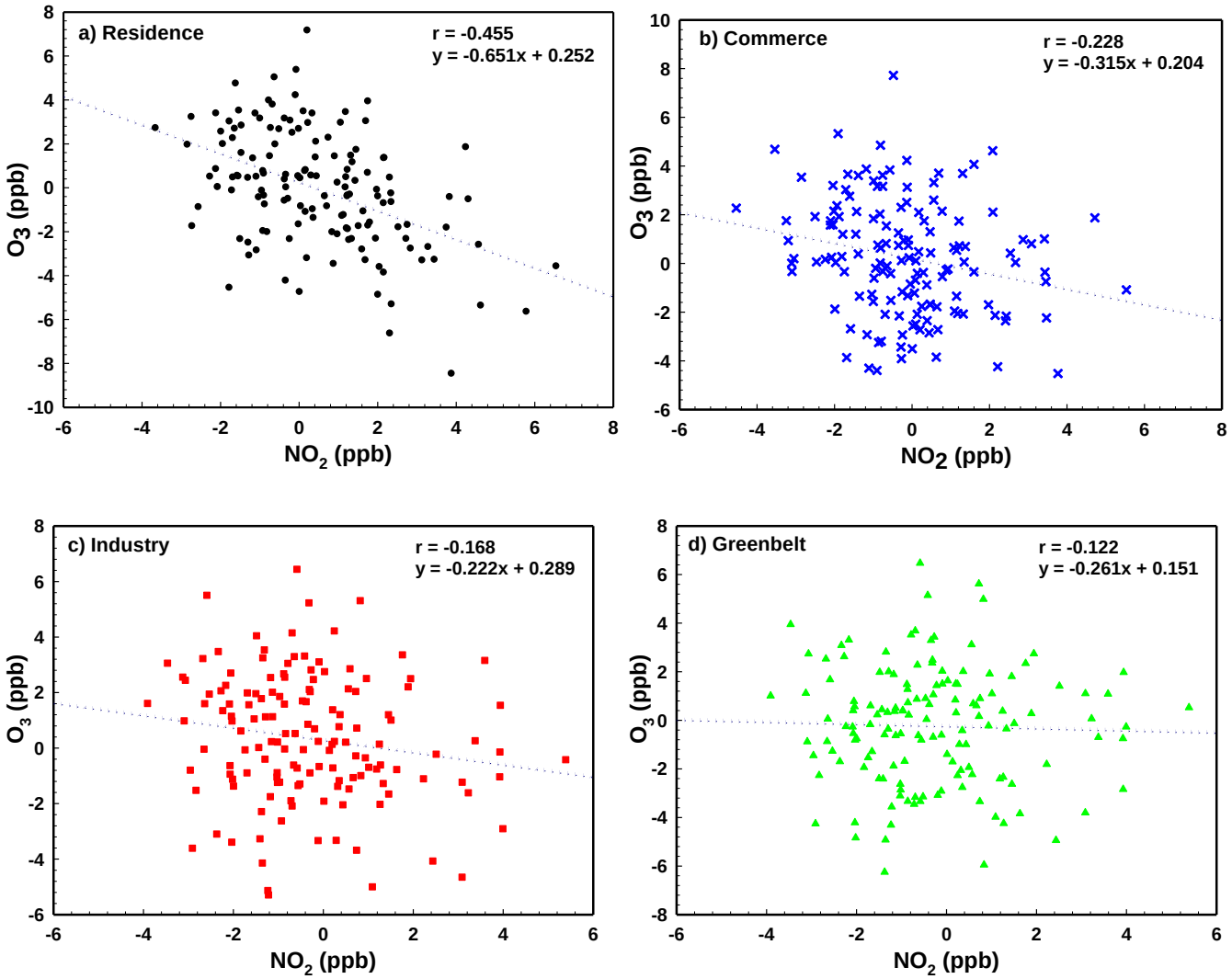

Fig. 8. Scatter diagrams of the monthly anomalies of O_3 (ppb) versus NO_2 (ppb) in South Korea during the period from January 2002 to December 2013 under the four land-use types; a) residence (black circle), b) commerce (blue cross), c) industry (red square), and d) greenbelt (green triangle). The correlation coefficient (r) and the regression dotted line are also given.

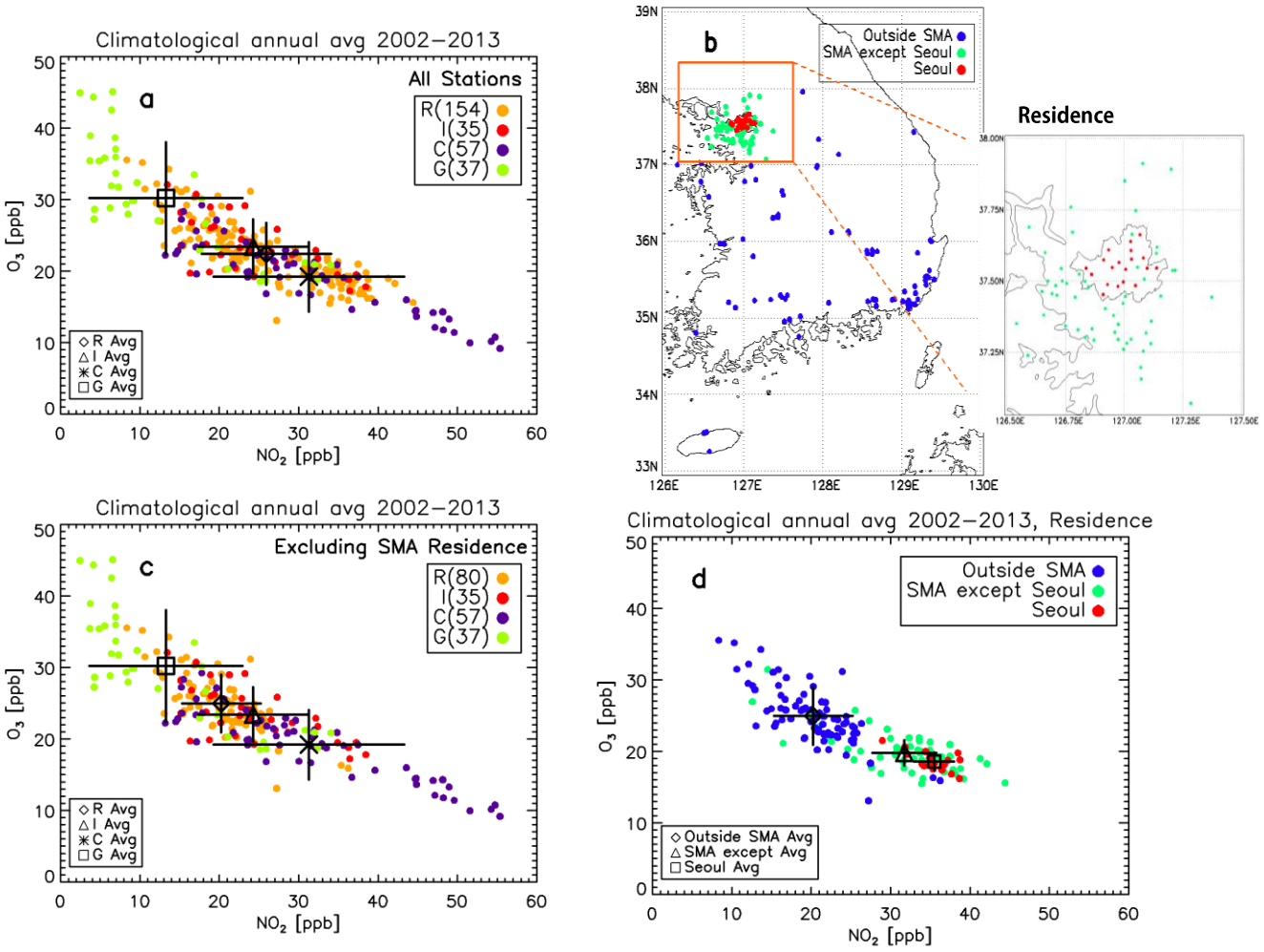

Fig. 9. Climatological annual averages of the O_3 (ppb) versus NO_2 (ppb) over South Korea during 2002-2013 under the MEK four land-use types of residence (R), commerce (C), industry (I), and greenbelt (G). a) O_3 versus NO_2 at whole 283 stations in South Korea. The number in the upper-right side panel of the figure indicates the count of stations. b) Locations of 154 'residence-type' stations subdivided by the three regions as follows; ⅰ) Seoul (red circle), ⅱ) the Seoul Metropolitan Area (SMA; green circle) except for Seoul, and ⅲ) outside of the SMA (blue circle). The rectangular area in Fig. 9b indicates that the SMA has been enlarged on the right side. c) Same as Fig. 9a except for excluding the O_3 and NO_2 observations of the SMA residential region. d) Same as Fig. 9a except for using the O_3 and NO_2 only in the 'residence' type under the three different regions of Fig. 9b. The mean values and standard deviations for the annual values of NO_2 and O_3 in each of the types are indicated in Figs. 9a, b, and d.

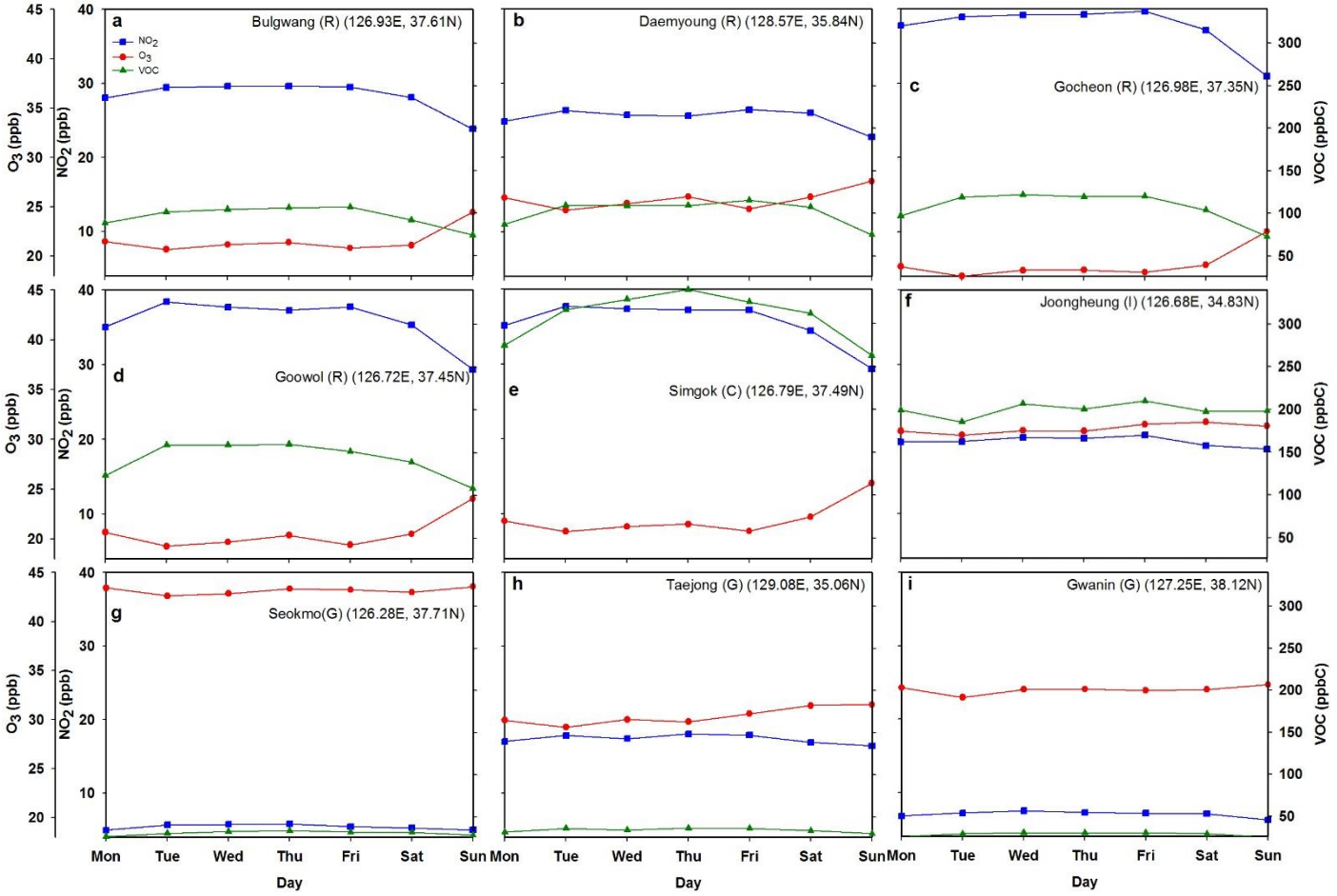

Fig. 10. The weekly variations in the VOCs (green triangle), O_3 (red circle), and NO_2 (blue rectangle) concentrations at the 9 photochemical air pollution monitoring stations in South Korea since 2007 under the MEK four land-use types as follows; residence (R), commerce (C), industry (I), and greenbelt (G). Please see Table 1 for the observational period at each of the VOCs station. For convenience, the terminology of 'VOC' in the figures means 'VOCs' in the text.

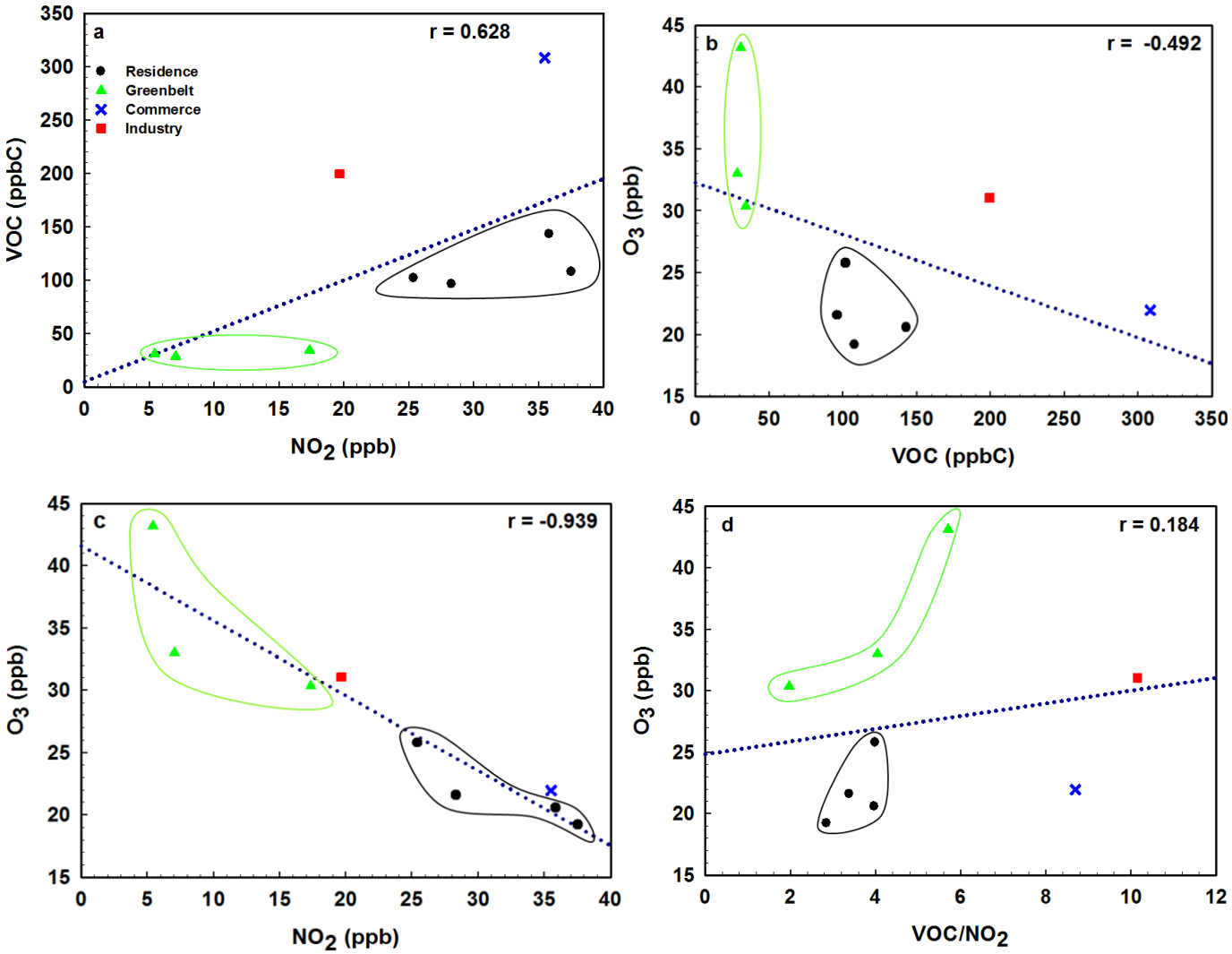

Fig. 11. Scatter diagrams of the long-term averages of a) VOCs versus NO_2, b) O_3 versus VOCs, c) O_3 versus NO_2, and d) O_3 versus the ratio of VOCs/NO_2 at 9 of the photochemical air pollution monitoring stations over South Korea since 2007 under the following four land-use types; residence (black circle), commerce (blue cross), industry (red square), and greenbelt (green triangle). The correlation coefficient (r) and the regression dotted line were also given.

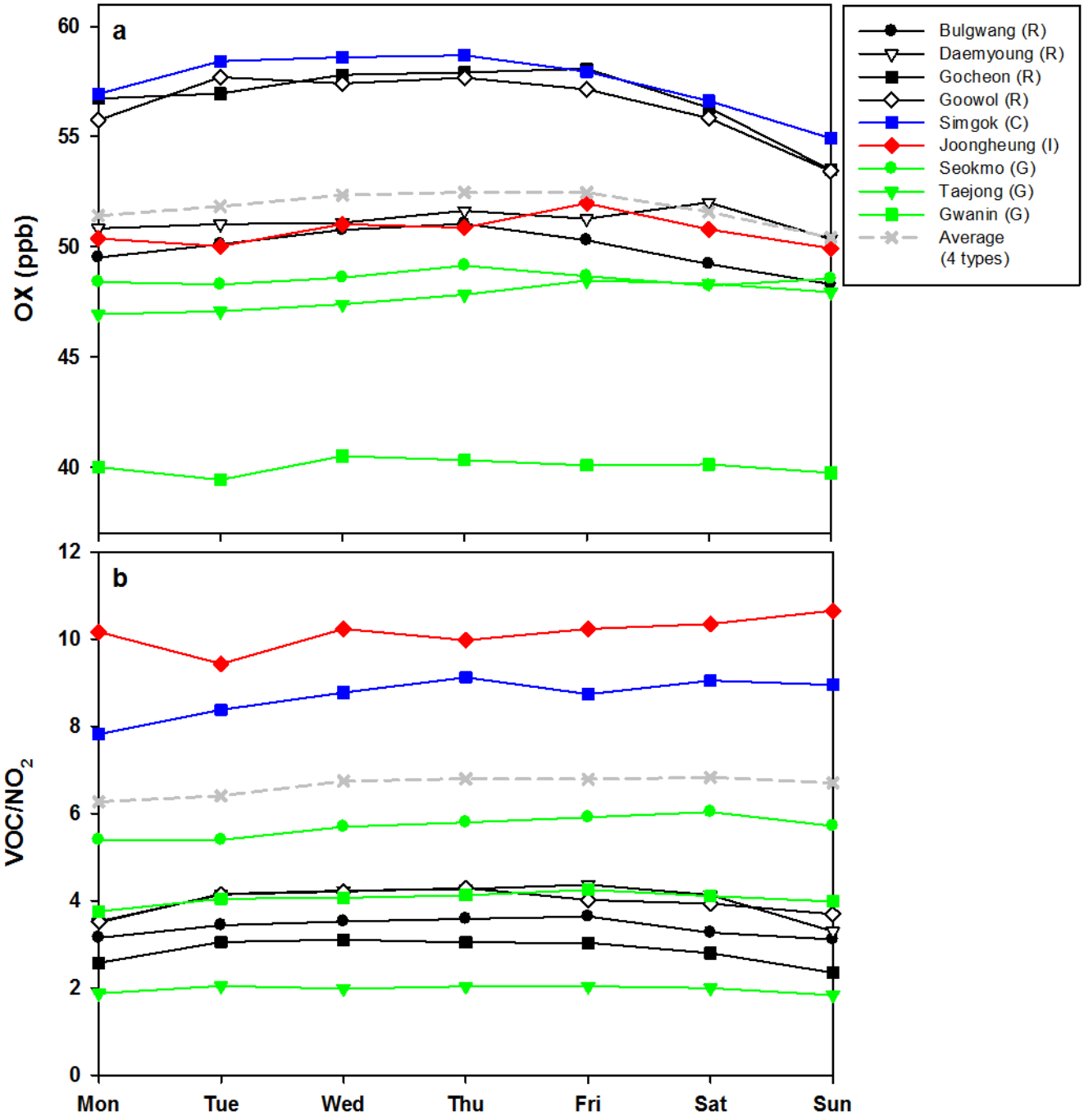

Fig. 12. Weekly variations in the a) OX and b) VOCs/NO_2 values 2007 at nine of the photochemical air pollution monitoring stations of the MEK in South Korea. Please see Table 1 for the observational period at each of the VOCs stations.

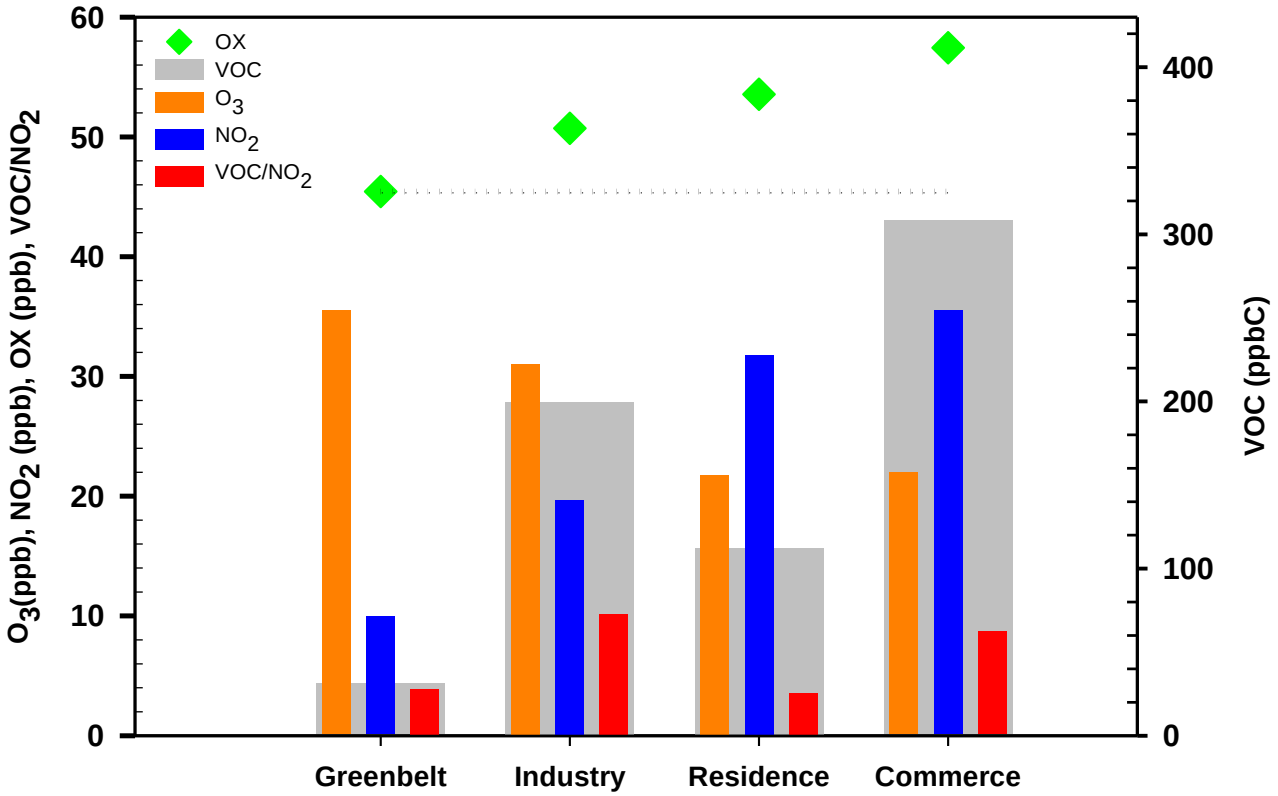

Fig. 13. Climatological averages of the OX (ppb), VOCs (ppbC), O_3 (ppb), NO_2 (ppb) and the ratio of VOCs/NO_2. The values of the VOCs, O_3, NO_2, and the ratio in the bar graph are shown in the colors of grey, scalet, blue and red, respectively, at 9 of the photochemical air pollution monitoring stations over South Korea since 2007 under the following MEK four land-use types of residence, commerce, industry, and greenbelt. The OX values are presented as green diamonds. Please see Table 1 for the observational period at each of the VOCs station.